Journal of Thermal Analysis and Calorimetry
https://doi.org/10.1007/s10973-025-14146-3

On the evaluation of thermomechanical parameters for caloric investigation of NiMnGaCu polycrystalline alloy

Corrado Tomasi[1] · Marco Evangelisti Crespo[3] · Elías Palacios[3] · David Gracia[3] · Francesca Villa[2] · Francesca Passaretti[2] · Elena Villa[2]

Received: 16 September 2024 / Accepted: 18 February 2025
© The Author(s) 2025

Abstract
Ferromagnetic shape memory alloys have received much attention for their multicaloric effect, in particular for their magnetocaloric/elastocaloric synergic coupling. Among them, NiMnGaCu alloys represent one of the most promising systems in terms of high magnetocaloric entropy change values. Our previous studies were addressed to assess the effect of microstructure on the elastocaloric effect. In the present work, a critical comparison among experimental data from different methodologies, i.e. DSC, adiabatic calorimetry under magnetic field, magnetization and thermomechanical measurements is made. The different approaches are discussed in terms of experimental and theoretical critical aspects.

Keywords Ferromagnetic shape memory alloys · Multicaloric effect · NiMnGaCu

Introduction

Because of the environmental problems and the increasing worldwide energy request, in the last decades solid state refrigeration technologies have received rising attention, thanks to their high efficiency and environmental friendliness [1]. In fact, there is both a great interest to replace the harmful volatile hydrofluorocarbon fluids used in vapour compression conventional refrigeration and overcome the problem of how miniaturize cooling devices for their use in electronics [2].

Solid state refrigeration is based on caloric effects that are expressed by both isothermal entropy change (ΔS_T) and adiabatic temperature change (ΔT_{ad}). Such quantities are triggered by the change of intensive parameters as magnetic field (leading to magnetocaloric effect), uniaxial stress (elastocaloric effect), electric field (electrocaloric effect), and hydrostatic pressure (barocaloric effect).

The magnetocaloric effect can be determined by both indirect methods, i.e. from magnetization measurements and/or field dependent heat capacity, and direct measurements. Direct experimental techniques commonly allow to obtain only the adiabatic temperature change and

✉ Corrado Tomasi
corrado.tomasi@cnr.it

Marco Evangelisti Crespo
evange@unizar.es

Elías Palacios
elias@unizar.es

David Gracia
davidg@unizar.es

Francesca Villa
francesca.villa@icmate.cnr.it

Francesca Passaretti
francesca.passaretti@cnr.it

Elena Villa
elena.villa@cnr.it

[1] Consiglio Nazionale delle Ricerche – Istituto della Materia Condensata e di Tecnologie per l'Energia (CNR-ICMATE Sede di Genova) Area della Ricerca di Genova, Via De Marini 16, 16149 Genoa, Italy

[2] Consiglio Nazionale delle Ricerche – Istituto della Materia Condensata e di Tecnologie per l'Energia (CNR-ICMATE Sede di Lecco), Via G. Previati 1/e, 23900 Lecco, Italy

[3] Department of Condensed Matter Physics and Instituto de Nanociencias y Materiales de Aragón (INMA), CSIC–University of Saragossa, Pedro Cerbuna 12, 50009 Zaragoza, Spain

Published online: 18 April 2025

can be carried out using contact and non-contact methods between the sample and the temperature sensor. However, Palacios et al. [3] developed precise techniques to determine directly both ΔT_{ad} and ΔS_T (in particular ΔS_T), in PPMS and adiabatic calorimeters. In any case, the accuracy of direct determinations mainly depends on the quality of thermal insulation of the sample as well as errors in thermometry and field setting. The indirect methods allow the calculation of just the isothermal entropy change by magnetization measurements or both ΔT_{ad} and ΔS_T by heat capacity measurements under magnetic field. In the former case the accuracy of the MCE is significantly linked to the correctness of the experimental procedure and, in minor extent, to the accuracy of the magnetic field, magnetic moment and temperature measurements, while in the latter it is critically dependent on the heat capacity determinations and related data processing.

A promising solid state refrigerant should exhibit ΔS_T and ΔT_{ad} with the following features: (1) high values, by applying low field change, (2) wide temperature spans near the selected refrigeration temperature, (3) high reversibility (i.e., slight hysteresis losses). Currently, meet all these requirements at the same time is a hard task. For instance, a wide range of materials exhibit the so called "giant caloric effect" that is typically associated with a first-order phase transition involving a noteworthy latent heat. The nature of such a first-order transition entails hysteresis that, as afore mentioned, represents an issue and lessens the refrigerant capacity of the material [4]. On the other hand, ferromagnets with second-order transitions usually exhibit limited MCE. Hence, when using first-order transition materials one has to try to reduce the unavoidable hysteresis to an acceptable small value.

Among potential candidates for solid state refrigeration, Heusler's type ferromagnetic shape memory alloys (FSMAs) are considered of great interest and have been investigated by many research groups [5–11]. In particular, the Ni_2MnGa-based Heusler alloys are important, since the partial replacement of Mn with Cu lowers the Curie temperature and shifts the martensitic transition toward higher temperatures [12–20]. In such a way, it is possible to tune the austenite transformation temperature to the ferromagnetic Curie temperature leading to the structural/magnetic coupling.

Over the last two decades lots of papers were addressed to the magnetic [21, 22] and caloric properties of the NiMnGaCu system and most of them focused on the magnetocaloric characterisation by measuring the isothermal entropy change via isothermal magnetization [16, 17, 20–24], while only few works have been devoted to determine the adiabatic temperature change [25, 26].

Quite recently, a noteworthy study was published by Gràcia Condal et al. [27], who focused their work on the magneto-mechanical coupling in NiMnGaCu through calorimetric measurements under magnetic field and controlled stress. The authors reported that at 299 K a $\Delta S_T = -14$ J kg^{-1} K^{-1} recorded with a magnetic field of ~ 2.5 T can be achieved at 1 T when a uniaxial stress of 12 MPa is applied. Similarly, at $T = 297$ K, a magnetic field of 6 T yields a ΔT ~ 6.5 K, whereas a value of 9.2 K is achieved when an additional stress of 20 MPa is applied.

Lately, Li et al. [28] investigated the magnetocaloric properties of $Ni_{50}Mn_{18.5}Ga_{25}Cu_{6.5}$ (at.%) Heusler alloy. They reported that a unique synergic feature of the alloy resulted in a phase transformation entropy change of -1.05 J mol^{-1} K^{-1}, in which the structural component accounts for ~ 63% and the magnetic component primarily contributes the remaining ~ 37%. By applying the Landau model, the authors theoretically simulated the ΔS_m of the alloy and found that it increases with magnetic field thanks to the synergic feature of the structural and magnetic components. By means of a unique device they also measured the adiabatic temperature change and found values up to 6.5 K under a magnetic field of 8 T.

The cyclic reversibility of martensitic transformation and the magnetocaloric effect in a $Ni_{51.0}Mn_{20.8}Ga_{22.4}Cu_{5.8}$ alloy has been investigated by Su et al. [29]. According to the authors, the martensitic transformation exhibits small thermal and magnetic hystereses (~6 K and ~6.8 J kg^{-1}, respectively) and excellent reversibility upon 50 thermal and magnetic cycles owing to the good geometric compatibility of the martensite/austenite transferring interface, with a reversible ΔS_m up to -21.7 J kg^{-1} K^{-1} achieved after 50 magnetic cycles under 50 kOe.

Zhang et al. [30], have successfully prepared Ni–Mn–Ga/Cu magnetocaloric composites via spark plasma sintering (SPS) by using ball-milled and heat-treated Ni–Mn–Ga alloy particles mixed with Cu powders. XRD patterns and EDS mapping indicated partial atomic diffusion, widened with increasing the sintering temperature. The authors, by applying the Curie–Weiss fitting found ferro-paramagnetic transition temperatures of 289–300 K and reported $-\Delta S_m$ up to 3 J kg^{-1} K^{-1} with broadened T_{FWHM} of 92 K, larger than that of many micro/nano-sized magnetocaloric materials, along with a maximum coefficient of thermal conductivity of 11.2 W m^{-1} K^{-1}. The application of a modified Hasselman–Johnson (H–J) model was used by the authors to correlate the thermal conductivity to the microstructure of the composite. The compression experiments carried out on Ni–Mn–Ga/Cu composites displayed a minimum fracture stress of 340 MPa and fracture strain of 4%, respectively, much better than that of bulk Ni–Mn–Ga alloys produced by arc-melting. (The composite failure mechanism was explained by finite element (FE) simulation based on the extended linear Drucker–Prager model). An improved magnetocaloric effect (MCE) of $Ni_{50}Mn_{18}Cu_7Ga_{25}$ through

unidirectional compression on the directionally solidified alloy was described by Zou et al. [31]. The induced preferred orientation and intermartensitic transformation led to a stronger coupling of magnetic-structural transition, and to more diverse transformation path, both enhancing ΔT_{ad} (up to -2.34 K at 1.5 T). The authors reported that the partial overlapping of the two transitions, coupling of intermartensitic transformation (CMIT) and coupling of martensitic transformation (CMMT), widens the magnetocaloric temperature range up to 7 K.

In our previous works [32, 33] we thermally, mechanically and structurally characterised samples with $Ni_{50}Mn_{18.5}Cu_{6.5}Ga_{25}$ chemical composition and explored how microstructure, induced by means of selected thermal treatments, affects the elastocaloric properties and the magnetocaloric response obtained by magnetization measurements. We also studied the effect of thermoelastic martensitic transformation (TMT) on the total entropy change and correlated to the C_{Ef} parameter, representing the efficiency of TMT. In these recent works attention has been focused on the evaluation of different contributions to the final ΔS, in particular the *mass* and the influence of TMT were highlighted. Magnetization and elastocaloric assessments were used to split the whole entropy change into magnetic and TMT contributions. Actually, the elastocaloric measurements, throughout mechanical tests allow to estimate the entropy change only due to the TMT. The comparison among samples with different efficiency in TMT confirms that the contribution of TMT to the total entropy change is the most significant [28].

The present work aims to face the caloric properties of the inspected system with an exhaustive approach from multiple points of view. NiMnGaCu has been investigated by means of various techniques and the obtained results critically compared and examined. An extensive discussion on both experimental data and possible flows affecting results for each experimental approach is also made, with the purpose of providing an analytical summary frame between experimental evidence and theory and a possible guideline for the correct use and interpretation.

Experimental

Materials

$Ni_{50}Mn_{18.5}Ga_{6.5}Cu_{25}$ alloy samples were melted by an arc furnace in Ar atmosphere (Leybold LK6/45) starting from pure elements (> 99%). The obtained ingots were re-melted six times in water-cooled copper crucible to guarantee chemical homogeneity. The following thermal treatments were chosen for optimization of grains structure according to our previous investigation: TT at 1123 K for 6 h under vacuum conditions followed by slow cooling (≈ 1 K min^{-1}) down to room temperature ("A" series samples) and TT at 1123 K for 12 h in Ar atmosphere followed by water quenching ("B" series samples). The mechanical features yielded by these thermal routes are acceptable and promising for elastocaloric characterization.

Methods

Q200 TA Instruments differential scanning calorimeter DSC, equipped by liquid nitrogen cooling system was used for calorimetric analysis. The measurements were carried out in the $223 \div 370$ K temperature range at a rate of 2 K min^{-1} under purge gas (He, 25 mL min^{-1}). The heat capacity measurements were performed by means of an adiabatic calorimeter AK-6.25, originally designed to measure heat capacity by the classical method of heat pulse. An original method, called "Thermogram" and specially designed to measure first-order transitions, was applied [3, 34]. It consists on quasi-static continuous heating or cooling under a constant magnetic field at typical rates of ± 100 mK min^{-1}. Mechanical tests were carried out with an E3000 Instron equipment fitted with a thermal control chamber in compression configuration. The elastocaloric adiabatic temperature measurements were obtained by a customized setup, with *T*-type thermocouples controlled by Labview (2020 community edition) software program. Magnetization measurements were performed by means of a commercial DC-SQUID magnetometer (MPMS2) by Quantum Design with applied magnetic fields up to 5.5 T and in the temperature range $300 \text{ K} < T < 360$ K.

Results

Figure 1 shows the heat capacity of samples A and B in the 300–360 K temperature range. C_p curves were obtained by elaborating accurate DSC measurements at 2 K min^{-1} repeated at least 3 times. Every measurement was performed by setting 10 min isotherms at the beginning and at the end of the scan, taking care of recording both baseline and sapphire traces at the same experimental conditions just before every sample run. The overall error can be estimated of the order of 7%.

From the picture, one can soon observe that the changes in microstructure reflect onto both the temperature and the shape of TMT. Further, both samples A and B exhibit heat capacity values higher for the martensite phase than those for the austenite one.

The present C_p values, although somewhat larger than the ones reported in our previous paper [32] are in

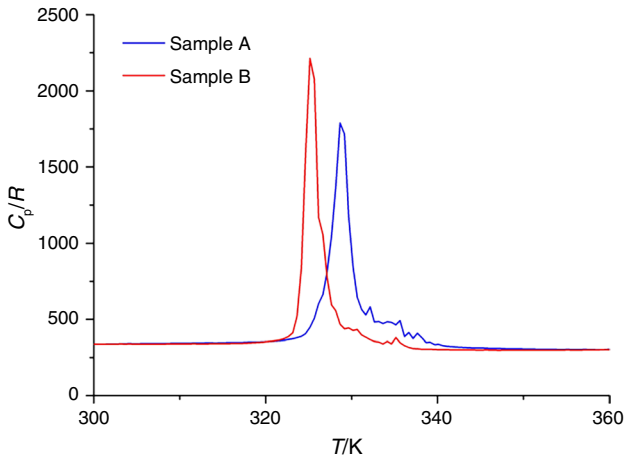

Fig. 1 Heat capacity versus T for samples A and B obtained on heating by DSC. The results are expressed in R units and refer to 100 atoms per formula

good agreement with the Dulong and Petit's law and, for temperatures below the TMT, coherent with the heat capacity of the close related $Ni_{50}CoMn_{36}Sn_{13}$ Heusler alloy [35].

As reported on our previous paper [33], the entropy change ΔS_{TMT} during the thermoelastic martensitic transformation can be calculated as $\Delta S_{TMT} = \Delta H/T_0$, where ΔH is the enthalpy variation measured in the calorimetric analysis. T_0, in turn, is defined as $T_0 = (Af + Ms)/2$, where Af stands for the Austenite phase finish temperature and Ms the Martensitic phase start temperature. Similarly, the temperature change, ΔT, given by the theoretical approach from calorimetric analysis can be calculated as $\Delta T = \Delta H/C_p$, where C_p is the specific heat obtained by calorimetric analysis. In both cases, the above parameters express the contribution related to the thermoelastic martensitic transformation, only.

Figure 2 reports the C_p values for sample A and B measured on heating and cooling by the Thermogram method applied to the adiabatic calorimeter under different magnetic fields (0, 3, 5 T). Although the transition temperatures by Thermogram seem not to agree with the DSC ones, one should consider that the heating rates applied in these two methods differ more than one order of magnitude. Also, it is worth noting that for both samples the specimen size analysed in the calorimeter (hundreds of mg) is smaller with respect to the sample mass commonly used (grams). However, significant results can be obtained by matching, at temperatures well below the martensitic transition, the heat capacity values from the adiabatic calorimeter with those coming from accurate and reliable DSC measurements.

The entropy has been computed from Thermogram as

$$S(T,B) = S\left(T_{ref},B\right) + \int_{T_0}^{T} \frac{C_{p,B}(T,B)}{T} dT \quad (1)$$

taking $T_{ref} = 335$ K, a temperature where the entropy is nearly field independent, since the sample is in paramagnetic austenite state. The isothermal entropy change, $\Delta S_T \simeq S(T, B) - S(T, 0)$, for samples A and B at 3 T and 5 T is shown in Fig. 3. One can notice that sample A exhibits peak max values somewhat higher than those of sample B on heating.

ΔT_{ad} in Fig. 4 has been obtained from heat capacity, via the entropy curves from the thermodynamic equation

$$\Delta S_T \equiv S(T,B) - S(T,0) = \int_{T}^{T+\Delta Ts} \frac{C_{p,B}(T,B)}{T} dT \quad (2)$$

The integral equation has been numerically solved for ΔT_S. In this procedure the adiabatic temperature increment

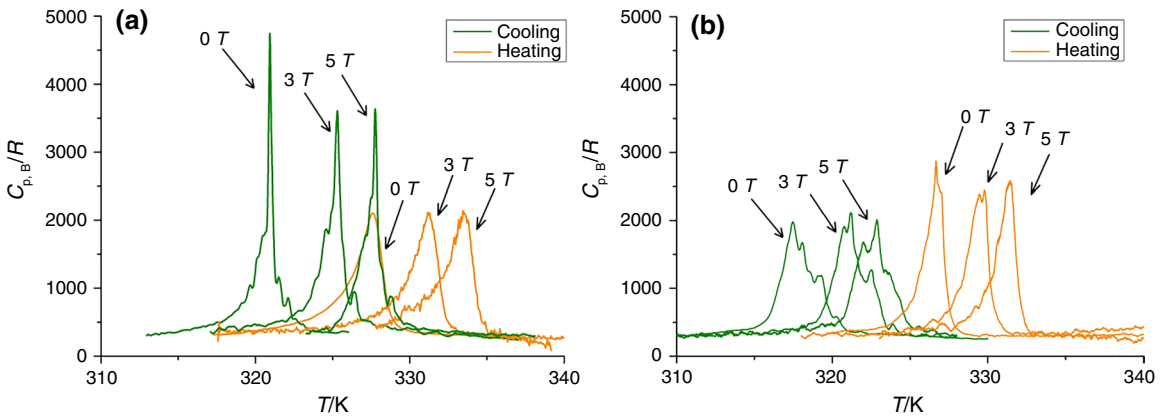

Fig. 2 Heat capacity versus T of samples A (left side) and B (right side) recorded on heating and cooling by adiabatic calorimetry under magnetic field

has been identified with the isentropic one. In this case $\Delta T_S > 0$, implies $\Delta T_{ad} > \Delta T_S$ according to the Second Law of Thermodynamics, but the difference is estimated in less than 0.1 K, that is less than the experimental errors. Both samples attain values around 4 K when a field of 5 T is applied. As in the case of ΔS_T, sample A displays peak max values up to 15% higher than those of sample B on heating, whereas are of the order of 40–50% higher on cooling.

From Figs. 3 and 4 it is apparent that sample A has higher ΔT_{ad} and ΔS_T values and better overall performance than sample B.

A more extensive comparison can be achieved by considering Table 1 [33] that resumes ΔS e ΔT data yielded

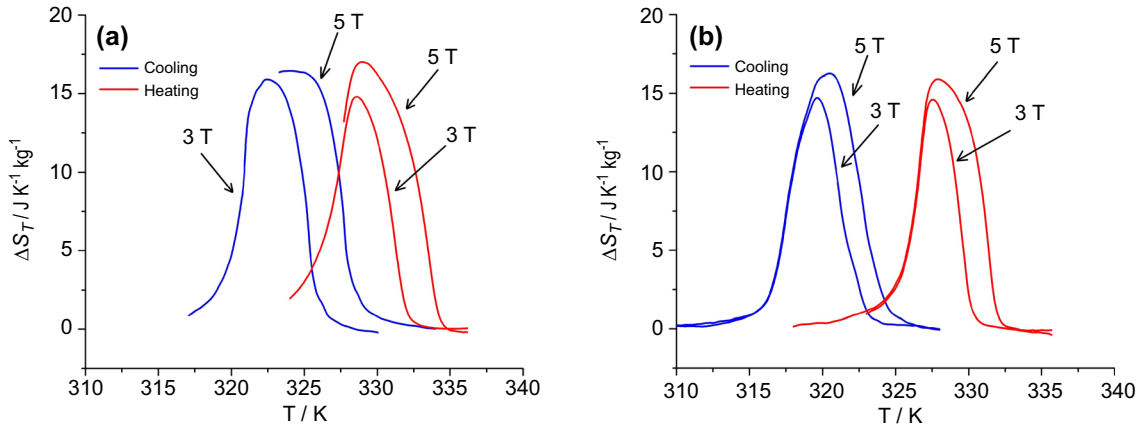

Fig. 3 Isothermal entropy change for samples A (left side) and B (right side) recorded on cooling and heating by applying the Thermogram method to the adiabatic calorimeter under different magnetic fields. The hysteresis between cooling and heating is ~ 6 K for sample A and ~ 8 K for sample B

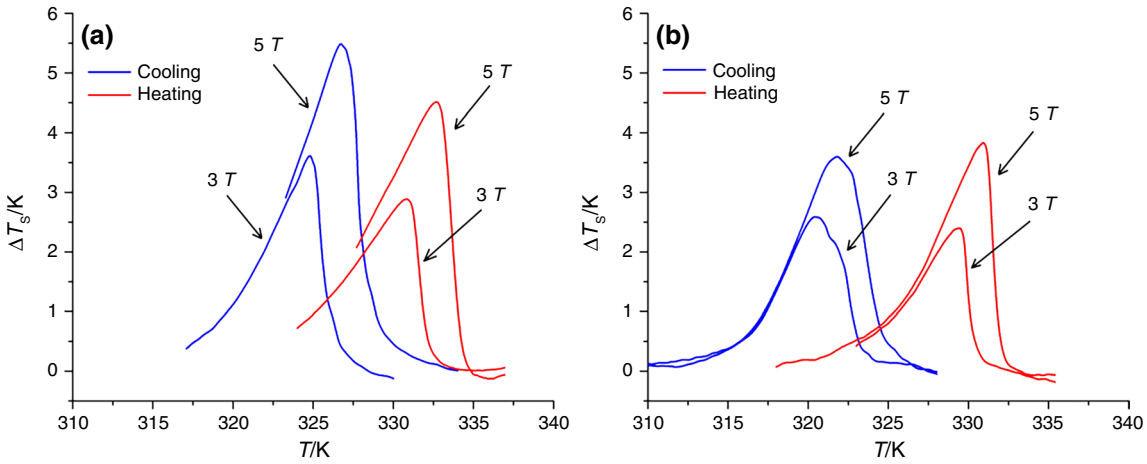

Fig. 4 Adiabatic temperature change for samples A (left side) and B (right side) recorded on cooling and heating by the Thermogram method applied to the adiabatic calorimeter under different magnetic fields. The hysteresis between cooling and heating is ~ 6 K for sample A and ~ 9 K for sample B

Table 1 Peak values and maximum values for ΔS and ΔT for the A and B sample series

	ΔS peak value cooling SR	ΔS peak value heating SR	ΔS peak value loading SS	ΔS peak value unloading SS	ΔT (DSC)	ΔT (exp)
A sample series	24.9	28.8	18.7	21.4	20.85	2.37
B sample series	36.9	55.9	27.7	34.1	24.5	4.5

The ΔS change values obtained by discrete integration are expressed in J kg^{-1} K^{-1}, the ΔT values are expressed in K

by elastocaloric measurements by both stress–strain (SS) and strain recovery (SR) approaches. According to Table 1, there is a similar trend for the two sets of data although a good agreement on absolute values is not found. It is not wrong to highlight that such a comparison is among entropy change values obtained by different driving forces. Each approach considers the TMT, but in elastocaloric step the induction of martensite is influenced by mechanical properties and general microstructure of the sample. In any case, the values obtained by DSC can be considered as an upper limit for the ΔT values [36]. A huge difference in both ΔT_{ad} e ΔS_T, according to the experimental method employed, is a characteristic of materials showing first-order transitions. Detailed studies on such an aspect, including comparisons with different techniques, is reported by Palacios et al. on $(MnNiSi)_{0.56}(FeNiGe)_{0.44}$ [3] and by Tocado et al. on MnAs [37]. In both papers the authors demonstrated that the most reliable information about the magnetocaloric parameters could be obtained by measuring the heat capacity under different magnetic field in an adiabatic calorimetry following the Thermogram method.

Figure 5 depicts the isothermal entropy change obtained by magnetization measurements already reported in our previous paper [32]. Despite the difference in the peak max temperature for sample A and B, the maximum ΔS values for each applied magnetic field are very similar.

Both the magnetocaloric and elastocaloric ΔS_T in Fig. 5 and Table 1, respectively, were computed by applying the well-known Maxwell relation

$$\left(\frac{\partial S}{\partial B}\right)_T = \left(\frac{\partial M}{\partial T}\right)_B \Rightarrow S(T,B) - S(T,B=0) = \Delta S_T = \int_0^B \left(\frac{\partial M}{\partial T}\right)_B dB \tag{3}$$

in case of magnetization and

$$\left(\frac{\partial S}{\partial \sigma}\right)_T = \left(\frac{\partial \varepsilon}{\partial T}\right)_\sigma \Rightarrow S(T,\sigma) - S(T,\sigma=0) = \Delta S_T = \int_0^\sigma \left(\frac{\partial \varepsilon}{\partial T}\right)_\sigma d\sigma \tag{4}$$

in case of stress and strain and strain recovery measurements.

Discussion

The optimization of the TMT by microstructural tuning is one of the best route to efficient the caloric effect driven by different fields. In particular, the use of mechanical solicitation allows to reduce the magnetic field involved in coupling of magnetic and mechanical driving force for caloric effect.

The discrepancy between the martensitic elastocaloric potential performance and its expression and evaluation in applications is clearly evident when comparing the ΔT values calculated from enthalpy and calorimetric measurements with those obtained from experimental mechanical curves: in this case the total heat transfer associated with the full stress-induced martensitic transformation is affected by structural defects and energy dispersion due, in turn, to the actual microstructure. Besides, the adiabatic ΔT_{ad} is strongly influenced by the sample geometry and the heat transmission efficiency. Indeed, in the current case the samples working between two compression platens were characterised by a low surface/volume ratio and this surely affected the ΔT_{ad} direct measurements. Furthermore, the theoretical ΔT obtained from the calorimetric measurements is significantly higher (see Table 1) and can reasonably be considered as an intrinsic maximum value for the NiMnGaCu material. Nevertheless, both the theoretical and experimental adiabatic ΔT from mechanical measurements look coherent with the microstructural condition of the examined samples, since the B sample, having a better optimized microstructure, shows higher elastocaloric ΔT values, in contrast to what obtained

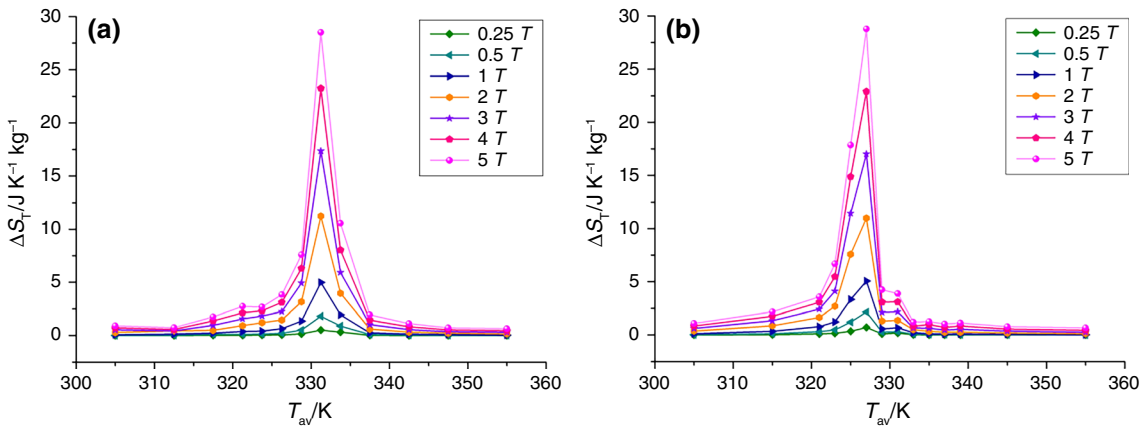

Fig. 5 Isothermal entropy change for samples A (left side) and B (right side) recorded on heating by magnetization under various magnetic fields [32]

from Thermogram method applied to the adiabatic calorimeter under magnetic field (Fig. 4).

By comparing the ΔS_T data of Table 1 with those of Fig. 5 one can observe a certain degree of disagreement. Such discrepancies are partially due to a fundamental reason. Being the entropy a thermodynamic state function, the ΔS_T evaluation obtained from magnetic and elastocaloric measurements is expected to be different because the entropy change from magnetic data is not determined between the same state points than for mechanical ones. In the former case ΔS_T is evaluated between (T, $B=0$, $\sigma=0$) and (T, B, $\sigma=0$), whereas in the latter case between (T, $B=0$, $\sigma=0$) e (T, $B=0$, σ). Moreover, both are affected by an overestimation related to the use of the Maxwell relation in a hysteric first-order transition material. The Maxwell relations reported above (Eqs. 3 and 4) are based on the mathematic theorem stating that $\left(\partial^2 G/\partial T\partial B\right)_\sigma = \left(\partial^2 G/\partial B\partial T\right)_\sigma$ (or $\left(\partial^2 G/\partial T\partial \sigma\right)_B = \left(\partial^2 G/\partial \sigma\partial T\right)_B$), i.e., the mixed second derivatives of the free energy are equal made in any order if both exist and are continuous. In case of first-order transitions, as for NiMnGaCu TMT, such conditions are not accomplished, since $S = (\partial G/\partial T)_{\sigma,B}$ and $\varepsilon = (\partial G/\partial \sigma)_{T,B}$ (or $M = (\partial G/\partial B)_{T,\sigma}$) are discontinuous. When dealing with hysteric first-order transition the Maxwell relation must be applied with caution or, more strictly speaking, the experimental procedure must be careful [37].

Hence, the usual protocol used for magnetization measurements to deduce ΔS_T via Maxwell relation (Eq. 3) does suffer some intrinsic errors that lead to wrong estimations of the magnetocaloric effect [3, 37]. The original Maxwell relation denotes that, under isothermal conditions, the entropy change on an infinitesimal magnetic field change is proportional to an infinitesimal change in magnetization at a constant magnetic field. An "infinitesimal" isothermal increment in magnetization is assumed when indeed the actual change is a magnetization to a very high field, demagnetization, heating to the new temperature T at zero field and the re-magnetization to the target B. In case of a hysteretic first-order transition this process is not equivalent to a simple small temperature increment at constant B, since the ferro/para fraction is very different, not infinitesimal.

Therefore, the ΔS values obtained by applying the Maxwell relation to both magnetization and mechanical sets of data are affected by significant errors called "spikes" that are proportional to the heat capacity at B (or σ) = 0 [3]. For example, Tocado et al. [37, 38] calculated the shape of the spike produced by the magnetization isotherms in the first-order transition of MnAs. Generally, in the Heusler alloys the spike smears over the whole T-range in which ΔS_T is large because the peak with of the heat capacity is comparable to the hysteresis.

It is known that in case of transitions with an associated hysteresis, in the range where two phases coexist in a metastable state, their ratio does not only depend on the magnetic field and temperature (or others intensive parameters such as pressure, etc.) but also on the previous sample history. Since at a given point (T, B) such a ratio is different according that it has been attained by heating or cooling, neither the entropy nor the enthalpy achieve the same values. Within the experimental error, the experimental entropy obtained from Eq. (1) coincides with its physico-statistic and thermodynamic definition.

Besides, the analysis of the entropy change in loading and unloading reveals differences in the corresponding values because of further aspects: the intrinsic non perfect symmetry between austenite–martensite (A to M) and martensite–austenite (M to A) transitions. In mechanical investigation the A to M transformation occurs by nucleation and detwinning of martensite, while the M to A transition takes place by shrinking of martensite, hence the resulting mechanical hysteresis reflects into a thermal hysteresis. Moreover, in the unloading stage (corresponding to M to A transition) the entropy change efficiency increases as a result of a more complete overlapping of *Tc* and *Af*. Due to these aspect, in fact, generally the entropy change reported in literature for this alloys is larger in heating part of magnetization curve or strain recovery curve or in unloading curves [20, 33].

The comparison between the isothermal entropy change determined by magnetic moment measurements and the Thermogram method for samples A and B depicted in Fig. 6 clearly shows that calorimetric ΔS_T is somewhat lower than that obtained by magnetization for all the applied magnetic fields. Although our ΔS_T values from magnetometry are in fairly good agreement with some results reported in literature [9, 23, 29] they are affected by the spike effect described above, whereas both ΔS_T and ΔT_{ad} from the Thermogram method are much more reliable. As described in the experimental session, the Thermogram method [3] used in this work is designed to study first-order transitions and consists of an adiabatic system, where the sample is continuously heated or cooled at a low rate (~ 2 mK s^{-1}). Though the most reliable and accurate calorimetric method is the traditional adiabatic calorimetry based on the classical heat pulse, in the present study it cannot be suitably applied because it works only on heating, is very time-consuming and, for every single measurement when assessing first-order transitions with phase coexistence, the relaxation time following a pulse tends to infinite. Hence, the caloric parameters from different experimental approaches are not always easy to compare.

It is worth stressing the following aspects:

– The optimization of the thermoelastic martensitic transformation is useful in order to maximise ΔS and ΔT related to the structural component that represent

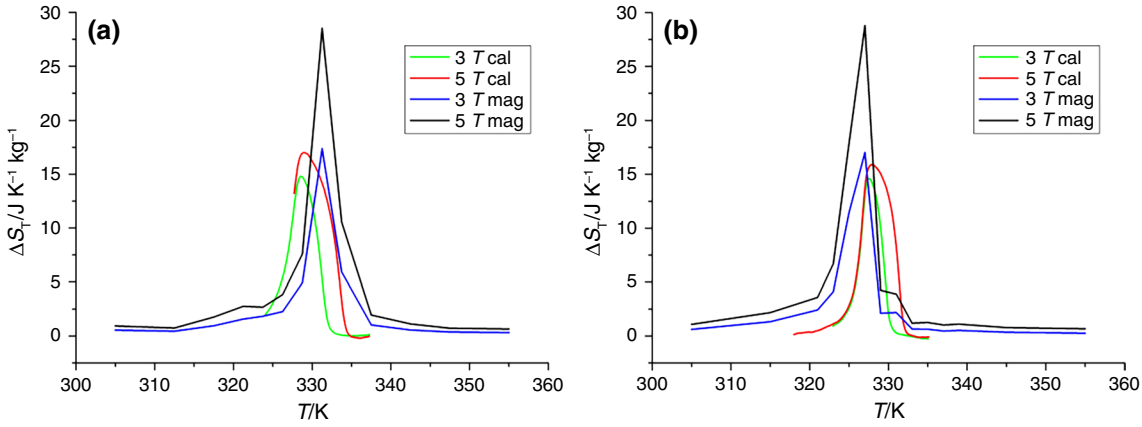

Fig. 6 Comparison between ΔS_T obtained by magnetization and Thermogram method (adiabatic calorimeter in heating) measurements under magnetic field of 3 and 5 T for sample A (left) and B (right)

the main contribution to the magnetostructural transformation.

- The isothermal entropy change values from specific heat measurements under magnetic field have to be considered more reliable than those obtained by the application of the Maxwell equation on magnetization data.
- Since, ΔS values from magnetization measurements are spurious because of the first-order transition hysteresis, one can hardly distinguish the A and B experimental curves that include the magnetic/structural coupling.

Conclusions

Magnetocaloric and elastocaloric properties of $Ni_{50}Mn_{18.5}Cu_{6.5}Ga_{25}$ were assessed from different points of view in order to critically compare the experimental results.

Among the envisaged techniques, the calorimetric analysis under applied magnetic field can be considered the best way to evaluate the magnetocaloric effect. A comparison with experimental ΔS_M values obtained by magnetization curves highlights how the first-order transition can produce overestimated magnetocaloric effect when the Maxwell equation is applied.

The elastocaloric analysis diverges from the calorimetric one because of a mechanical driving force inducing TMT that suffers from possible inhomogeneity and irregularity of the microstructure to a higher extent.

A further step to investigate the multicaloric performance of these materials can be represented by the magneto-mechanical coupling via application of moderate magnetic fields (up to 5 T).

Authors' contribution CT was involved in corresponding author, conceptualization, experimental, data analysis, and writing original draft. MEC was involved in experimental, data curation, review and editing. EP was involved in experimental, data curation, discussion (writing), review and editing. DG was involved in experimental, and data analysis. FV was involved in experimental. FP was involved in review and editing. EV was involved in conceptualization, experimental, data analysis, and writing.

Funding Open access funding provided by Consiglio Nazionale Delle Ricerche (CNR) within the CRUI-CARE Agreement.

Open Access This article is licensed under a Creative Commons Attribution 4.0 International License, which permits use, sharing, adaptation, distribution and reproduction in any medium or format, as long as you give appropriate credit to the original author(s) and the source, provide a link to the Creative Commons licence, and indicate if changes were made. The images or other third party material in this article are included in the article's Creative Commons licence, unless indicated otherwise in a credit line to the material. If material is not included in the article's Creative Commons licence and your intended use is not permitted by statutory regulation or exceeds the permitted use, you will need to obtain permission directly from the copyright holder. To view a copy of this licence, visit http://creativecommons.org/licenses/by/4.0/.

References

1. Hou H, Quian S, Takeuchi I. Materials, physics and systems for multicaloric cooling. Nat Rev Mater. 2022. https://doi.org/10.1038/s41578-022-00428-x.
2. Cazorla C. Novel mechanocaloric materials for solid-state cooling applications. Appl Phys Rev. 2019. https://doi.org/10.1063/1.5113620.
3. Palacios E, Burriel R, Zhang L. Calorimetric study of the giant magnetocaloric effect in $(MnNiSi)_{0.56}(FeNiGe)_{0.44}$. Phys Rev B. 2021. https://doi.org/10.1103/PhysRevB.103.104402.
4. Masche M, Ianniciello L, Tušek J, Engelbrecht K. Impact of hysteresis on caloric cooling performance. Int J Refrig. 2021. https://doi.org/10.1016/j.ijrefrig.2020.10.012.
5. Pasquale M, Sasso CP, Lewis LH, Giudici L, Lograsso T, Schlagel D. Magnetostructural transition and magnetocaloric effect in

$Ni_{55}Mn_{20}Ga_{25}$ single crystals. Phys Rev B. 2005. https://doi.org/10.1103/PhysRevB.72.094435.
6. Kainuma R, Imano Y, Ito W, Morito H, Sutou Y, Oikawa K, Fujita A, Ishida K, Okamoto S, Kitakami O, Kanomata T. Metamagnetic shape memory effect in a Heusler-type $Ni_{43}Co_7Mn_{39}Sn_{11}$ polycrystalline alloy. Appl Phys Lett. 2006. https://doi.org/10.1063/1.2203211.
7. Obradó E, Gonzàlez-Comas A, Mañosa L, Planes A. Magnetoelastic behavior of the Heusler Ni_2MnGa alloy. J Appl Phys. 1998. https://doi.org/10.1063/1.367620.
8. Khovailo VV, Abe T, Koledov VV, Matsumoto M, Nakamura N, Note R, Ohtsuka M, Shavrov VG, Takagi T. Influence of Fe and Co on phase transitions in NiMnGa alloys. Mater Trans. 2003. https://doi.org/10.48550/arXiv.cond-mat/0312639.
9. Cherechukin AA, Takagi T, Matsumoto M, Buchel'nikov VD. Magnetocaloric effect in $Ni_{2+x}Mn_{1-x}Ga$ Heusler alloys. Phys Lett A. 2004. https://doi.org/10.1016/j.physleta.2004.03.072.
10. Buchel'nikov VD, Zagrebin MA, Taskaev SV, Shavrov VG, Koledov VV, Khovaylo VV. New Heusler alloys with a metamagnetostructural phase transition. Bull Russ Acad Sci Phys. 2008. https://doi.org/10.3103/S1062873808040333.
11. Salazar-Mejìa C, Gomes AM, de Oliveira LAS. A less expensive NiMnGa based Heusler alloy for magnetic refrigeration. J Appl Phys. 2012. https://doi.org/10.1063/1.3675064.
12. Chernenko VA, Cesari E, Kokorin VV, Vitenko IN. The development of new ferromagnetic shape memory alloys in Ni-Mn-Ga system. Scr Metall Mater. 1995. https://doi.org/10.1016/0956-716X(95)00370-B.
13. Glavatskyy I, Glavatska N, Dobrinsky A, Hoffmann J-U, Söderberg O, Hannula S-P. Crystal structure and high-temperature magnetoplasticity in the new Ni–Mn–Ga–Cu magnetic shape memory alloys. Scr Mater. 2007. https://doi.org/10.1016/j.scriptamat.2006.12.019.
14. Wang J, Bai H, Jiang C, Li Y, Xu H. A highly plastic $Ni_{50}Mn_{25}Cu_{18}Ga_7$ high-temperature shape memory alloy. Mater Sci Eng A. 2010. https://doi.org/10.1016/j.msea.2009.12.021.
15. Santamarta R, Muntasell J, Font J, Cesari E. Thermal stability and microstructure of Ni-Mn-Ga-Cu high temperature shape memory alloys. J Alloy Compd. 2015. https://doi.org/10.1016/j.jallcom.2015.07.054.
16. Zhang X, Qian M, Zhang Z, Wei L, Geng L, Sun J. Magnetostructural coupling and magnetocaloric effect in Ni-Mn-Ga-Cu microwires. Appl Phys Lett. 2016. https://doi.org/10.1063/1.4941232.
17. Zhao D, Castán T, Planes A, Li Z, Sun W, Liu J. Enhanced caloric effect induced by magnetoelastic coupling in NiMnGaCu Heusler alloys: experimental study and theoretical analysis. Phys Rev B. 2017. https://doi.org/10.1103/PhysRevB.96.224105.
18. Mashirov AV, Irzhak AV, Tabachkova NY, Milovich FO, Kamantsev AP, Zhao D, Liu J, Kolesnikova VG, Rodionova VV, Koledov VV. Magnetostructural phase transition in micro- and nanosize Ni-Mn-Ga-Cu alloys. IEEE Magn Lett. 2019. https://doi.org/10.1109/LMAG.2019.2944585.
19. Planes A, Manosa L, Acet M. Magnetocaloric effect and its relation to shape-memory properties in ferromagnetic Heusler alloys. J Phys Condens Matter. 2009. https://doi.org/10.1088/0953-8984/21/23/233201.
20. Sarkar SK, Babu PD, Biswas A, Siruguri V, Krishnan M. Giant magnetocaloric effect from reverse martensitic transformation in Ni-Mn-Ga-Cu ferromagnetic shape memory alloys. J Alloys Compd. 2016. https://doi.org/10.1016/j.jallcom.2016.02.039.
21. Khan M, Dubenko I, Stadler S, Ali N. The structural and magnetic properties of $Ni_2Mn_{1-x}Ga$ (M=Co, Cu). J Appl Phys. 2005. https://doi.org/10.1063/1.1847131.
22. Jiang C, Wang J, Li P, Jia A, Xu H. Search for transformation from paramagnetic martensite to ferromagnetic austenite: NiMnGaCu alloys. Appl Phys Lett. 2009. https://doi.org/10.1063/1.3155199.
23. Gomes AM, Khan M, Stadler S, Ali N, Dubenko I, Takeuchi AY, Guimarães AP. Magnetocaloric properties of the $Ni_2Mn_{1-x}(Cu, Co)_xGa$ Heusler alloys. J Appl Phys. 2006. https://doi.org/10.1063/1.2164415.
24. Stadler S, Khan M, Mitchell J, Ali N, Gomes AM, Dubenko I, Takeuchi AY, Guimarães AP. Magnetocaloric properties of $Ni_2Mn_{1-x}Cu_xGa$. Appl Phys Lett. 2006. https://doi.org/10.1063/1.2202751.
25. Kaštil J, Kamarád J, Knížek K, Arnold Z, Javorský P. Peculiar magnetic properties of Er conditioned $Ni_{43}Co_7Mn_{31}Ga_{19}$ at ambient and hydrostatic pressures. J Alloys Compd. 2013. https://doi.org/10.1016/j.jallcom.2013.02.144.
26. McLeod MV, Bayer D, Turgut Z, Giri AK, Majumdar BS. Significant enhancement of magnetocaloric effect in a NiMnCuGa Heusler alloy through textural modification. J Appl Phys. 2020. https://doi.org/10.1063/5.0003366.
27. Gràcia-Condal A, Planes A, Mañosa L, Wei Z, Guo J, Soto-Parra D, Liu J. Magnetic and structural entropy contributions to the multicaloric effects in Ni-Mn-Ga-Cu. Phys Rev Mater. 2022. https://doi.org/10.1103/PhysRevMaterials.6.084403.
28. Li F, Zhao D, Liu J, Kamantsev A, Dilmieva E, Koshkid'ko Y, Zhu C, Ma L, Zhen C, Hou D. Entropy change of magnetostructural transformation and magnetocaloric properties in a $Ni_{50}Mn_{18.5}Ga_{25}Cu_{6.5}$ Heusler alloy. Mater Res Bull. 2023. https://doi.org/10.1016/j.materresbull.2022.112050.
29. Su M, Hou X, Zhang J, Zhao D, Zhen C, Ma L, Hou D. Cyclic reversible martensitic transformation and magnetocaloric effect in a $Ni_{51.0}Mn_{20.8}Ga_{22.4}Cu_{5.8}$ alloy. Mater Lett. 2023. https://doi.org/10.1016/j.matlet.2023.134592.
30. Zhang Y, Gao Y, Franco V, Yin H, Peng H-X, Qin F. Large thermal conductivity and robust mechanical properties of Ni-MnGa/Cu magnetocaloric composites prepared by spark plasma sintering. Sci China Mater. 2023. https://doi.org/10.1007/s40843-023-2491-6.
31. Zou N, Li D, Yang J, Wang H, Zhang L, Li Z, Wu B, Zuo L. Magnetocaloric performance optimized by simple compression in directionally solidified $Ni_{50}Mn_{18}Cu_7Ga_{25}$ alloy. J Alloys Compd. 2022. https://doi.org/10.1016/j.jallcom.2022.166001.
32. Villa E, Tomasi C, Nespoli A, Passaretti F, Lamura G, Canepa F. Investigation of microstructural influence on entropy change in magnetocaloric polycrystalline samples of NiMnGaCu ferromagnetic shape memory alloy. J Mater Res Technol. 2020. https://doi.org/10.1016/j.jmrt.2019.12.057.
33. Villa F, Bestetti E, Frigerio R, Caimi M, Tomasi C, Passaretti F, Villa E. Elastocaloric properties of polycrystalline samples of NiMnGaCu ferromagnetic shape memory alloy under compression: effect of improvement of thermoelastic martensitic transformation. Materials. 2022. https://doi.org/10.3390/ma15207123.
34. Palacios E, Melero JJ, Burriel R, Ferloni P. Structural, calorimetric, and Monte Carlo investigation of the order-disorder transition of BF_4 in $(CH_3)_4NBF_4$. Phys Rev B. 1996. https://doi.org/10.1103/PhysRevB.54.9099.
35. Palacios E, Bartolomé J, Wang G, Burriel R, Skokov K, Taskaev S, Khovaylo V. Analysis of the magnetocaloric effect in heusler alloys: study of $Ni_{50}CoMn_{36}Sn_{13}$ by calorimetric techniques. Entropy. 2015. https://doi.org/10.3390/e17031236.
36. Otsuka K, Ren X. Physical metallurgy of Ti–Ni-based shape memory alloys. Prog Mater Sci. 2005. https://doi.org/10.1016/j.pmatsci.2004.10.001.
37. Tocado L, Palacios E, Burriel R. Entropy determinations and magnetocaloric parameters in systems with first-order transitions:

study of MnAs. J Appl Phys. 2009. https://doi.org/10.1063/1.3093880.
38. Tocado L, Palacios E, Burriel R. Adiabatic measurements of the giant magnetocaloric effect in MnAs. J Therm Anal Calorim. 2006. https://doi.org/10.1007/s10973-005-7180-z.

Publisher's Note Springer Nature remains neutral with regard to jurisdictional claims in published maps and institutional affiliations.